Submitted to Metallurgical Transactions

UCRL-19029 Rev.
Preprint

c.2

INVESTIGATION OF THE CONVECTIVE-DIFFUSION LIMITED OXIDATION OF MOLYBDENUM BY THE ROTATING DISK METHOD

D. R. Olander and J. L. Schofill, Jr.

RECEIVED
LAWRENCE
RADIATION LABORATORY

SEP 17 1970

LIBRARY AND
DOCUMENTS SECTION

March 1970

AEC Contract No. W-7405-eng-48

TWO-WEEK LOAN COPY

This is a Library Circulating Copy
which may be borrowed for two weeks.
For a personal retention copy, call
Tech. Info. Division, Ext. 5545

LAWRENCE RADIATION LABORATORY
UNIVERSITY of CALIFORNIA BERKELEY

25

UCRL-19029 Rev.

DISCLAIMER

This document was prepared as an account of work sponsored by the United States Government. While this document is believed to contain correct information, neither the United States Government nor any agency thereof, nor the Regents of the University of California, nor any of their employees, makes any warranty, express or implied, or assumes any legal responsibility for the accuracy, completeness, or usefulness of any information, apparatus, product, or process disclosed, or represents that its use would not infringe privately owned rights. Reference herein to any specific commercial product, process, or service by its trade name, trademark, manufacturer, or otherwise, does not necessarily constitute or imply its endorsement, recommendation, or favoring by the United States Government or any agency thereof, or the Regents of the University of California. The views and opinions of authors expressed herein do not necessarily state or reflect those of the United States Government or any agency thereof or the Regents of the University of California.

INVESTIGATION OF THE CONVECTIVE-DIFFUSION LIMITED OXIDATION OF MOLYBDENUM BY THE ROTATING DISK METHOD

by D. R. Olander and J. L. Schofill, Jr.

Inorganic Materials Research Laboratory, Lawrence Radiation Laboratory
Department of Nuclear Engineering, College of Engineering
University of California, Berkeley, California

ABSTRACT

A rotating disk system has been developed to study heterogeneous chemical reactions subject to gas phase diffusion limitations. The system has been operated at temperatures up to 2000°K and disk speeds up to 15,000 rpm to investigate the reaction of oxygen and molybdenum. The independence of reaction or diffusion on radial position in the rotating disk system permitted kinetic data to be obtained from simple weight loss measurements as a function of disk temperature, oxygen partial pressure, and disk speed.

Because of the availability of an exact solution of the diffusion-convection equation for the rotating disk, the diffusional contribution to the overall rate can be accurately assessed when both gas phase diffusion and surface reaction offer resistances of comparable magnitude.

The results of this work demonstrated the importance of studying atmospheric pressure, high temperature heterogeneous reactions in a flow system for which accurate prediction of diffusional limitations is possible. The rotating disk is an eminently satisfactory tool for such theoretical and experimental studies.

The oxidation of molybdenum has been investigated by a variety of techniques over the past decade (1-6). The majority of these studies (3-6) were performed at high total gas pressures ($>\sim 50$ torr) where the oxidation rate is influenced by mass transfer in the gas adjacent to the surface. The results of these investigations have been reviewed by Rosner (7). The object of the present work was to measure the oxidation kinetics of molybdenum using low concentrations of oxygen in an inert diluent at a total pressure of 1 atm in a flow system in which the contribution of convective diffusion could be predicted theoretically. The importance of accurate assessment of gas phase diffusional resistance has been discussed by Rosner (8). The rotating disk method utilized in the present work has been applied previously to the germanium-iodine reaction (9).

Thermochemistry

Oxidation of molybdenum at temperatures greater than 1100°K proceeds by the overall reaction:

$$Mo(s) + \frac{3}{2} O_2(g) = \frac{1}{m} (MoO_3)_m(g) \qquad (A)$$

The 3/2:1 oxygen-to-molybdenum stoichiometry has been demonstrated by Gulbransen et al (4) and was verified in the present study. The average degree of polymerization of the product trioxide, m, ranges between one and three, depending upon the temperature and oxygen partial pressure in the reactant gas.

Between 1100 and 2000°K, a tough, adherent coat of MoO_2 is present on the oxidizing specimen. The oxide coat was observed in the present work and is evident in the photographs of oxidized specimens in ref 4. Solid state diffusion through this coat was not the primary resistance to oxidation; the oxidation rate was

time-independent under all conditions and at high temperatures, the rate was governed completely by oxygen mass transfer through the gas boundary layer. Nevertheless, the gas phase at the specimen surface was in contact with MoO_2, not molybdenum metal, and the following discussion of the thermodynamics of the reaction is based on this premise. Simple mass transfer theory and thermodynamic properties of the $Mo-O_2$ system are applied in a manner first described by Wagner (10) to answer the following questions:

(1) If all processes at the gas-solid interface are in equilibrium, and the rate of reaction is completely controlled by gas phase diffusion, is the oxygen partial pressure at the surface reduced to zero? In other words, are there chemical equilibrium restrictions to the diffusion-controlled rate?

(2) What is the degree of polymerization of the gaseous trioxide at the specimen surface?

(3) Under what conditions will the MoO_2 coat disappear and expose a bare metal surface to the reactant gas?

The two experimental parameters which are important in these computations are the surface temperature and the oxygen partial pressure in the bulk reactant gas. The mass transfer process is important in these considerations since it establishes a relation between bulk oxygen partial pressure, surface oxygen partial pressure, and the partial pressure of the molybdenum trioxide species at the surface.

Since both reactant oxygen and product trioxide constitute less than 5% of the total gas (the rest being an inert diluent), multi-component diffusional effects may be neglected and the rate of transport of oxygen to the solid surface described by:

$$N_{O_2} = k_{gO_2} \left(p^{\infty}_{O_2} - p^{0}_{O_2} \right) \tag{1}$$

where N_{O_2} is the number of moles of oxygen transported to the surface per cm^2 and per second, k_{gO_2} is the gas phase mass transfer coefficient of oxygen in the diluent gas and $p^{\infty}_{O_2}$ and $p^{0}_{O_2}$ are the partial pressures of oxygen in the bulk gas and the gas at the surface, respectively. According to the stoichiometry of reaction (A),

$$N_{O_2} = \frac{3}{2} N_{triox} \tag{2}$$

where N_{triox} is the number of gram atoms of molybdenum removed from the surface per cm^2 and per second as MoO_3, irrespective of its degree of polymerization. Transport of the product trioxide through the boundary layer is accompanied by the polymerization reactions:

$$2\ MoO_3(g) = (MoO_3)_2(g) \tag{B}$$

and

$$3\ MoO_3(g) = (MoO_3)_3(g) \tag{C}$$

The degree of polymerization depends upon the temperature and the total MoO_3 pressure:

$$p_T = p_1 + p_2 + p_3 \tag{3}$$

where p_1, p_2, and p_3 are the partial pressures of the monomer, dimer, and trimer, respectively. Higher polymers are not considered. Since p_T is largest at the specimen surface and decreases to zero at the outer edge of the gas boundary layer, and since the temperature also decreases through the boundary layer, the degree of polymerization

changes along the diffusion path. If the diffusion coefficients of the three polymers were known and reactions (B) and (C) were at local equilibrium at all points in the gas boundary layer, the rotating disk diffusion-convection equations for the three species could be solved. However, since the diffusion coefficients are not known, and since the solution of non-linear differential equations would be required, we adopt the simplification that the diffusivities of all three trioxide species are equal. This assumption implies that the transport behavior of the product oxide is independent of the local state of polymerization, or that for the purpose of computing transport rates, all gaseous oxide can be treated as monomer. Although the equal diffusivity approximation precludes accurate evaluation of the effect of polymerization on the product transport rate, it permits simple and probably sufficiently accurate computation of the roles of reactant and product transport in the overall oxidation process.

With the equal diffusivity assumption, the rate of trioxide transport in the gas boundary layer can be described by the product of a mass transfer coefficient and the surface partial pressure of the volatile oxide if it were all in the form of monomer:

$$N_{triox} = k_{gMoO_3} \left(p_1^0 + 2p_2^0 + 3p_3^0\right) \tag{4}$$

Combining Eqs (1), (2), and (4) yields the desired relation between the partial pressures of oxygen in the bulk and at the surface and the surface partial pressure of the oxide polymers:

$$1 - \frac{p_{O_2}^0}{p_{O_2}^\infty} = \gamma \frac{p_T^0}{p_{O_2}^\infty} (x_1 + 2x_2 + 3x_3) \tag{5}$$

where x_1, x_2, and x_3 are the fractions of the gaseous oxide at the surface in the form of monomer, dimer, and trimer, respectively (i.e., $x_1 = p_1^0/p_T^0$, etc.). The parameter γ is 3/2 times the ratio of the mass transfer coefficients of the product oxide and oxygen. According to the theory of convective-diffusion on a rotating disk, the mass transfer coefficient is proportional to the square root of the diffusion coefficient, so that γ may be written as:

$$\gamma = \frac{3}{2}\left(\frac{D_{MoO_3}}{D_{O_2}}\right)^{1/2} \tag{6}$$

The diffusivity of MoO_3 in argon or helium is not known, but it is certainly smaller than that of oxygen. Consequently, the parameter γ is probably in the neighborhood of unity.

In order to determine the ratio of the oxygen partial pressures at the surface and in the bulk, the following equilibria are required:

$$MoO_2(s) = Mo(s) + O_2(g) \tag{D}$$

and

$$\frac{3}{2}\,MoO_2(s) = \frac{1}{2}\,Mo(s) + MoO_3(g) \tag{E}$$

Applying reactions (D) and (E) to the gas phase at the surface yields:

$$K_E/\sqrt{K_D} = p_1^0/\sqrt{p_{O_2}^0} = x_1\ p_T^0/\sqrt{p_{O_2}^0} \tag{7}$$

where K_D and K_E are the equilibrium constants of reactions (D) and (E) respectively.

Utilizing the equilibrium constants of reactions (B) and (C) (denoted by K_B and K_C, respectively), the degree of polymerization

is determined by solution of:

$$1 = x_1 + \left(K_B p_T^0\right) x_1^2 + \left[K_3\left(p_T^0\right)^2\right] x_1^3 \tag{8}$$

$$x_2 = \left(K_B p_T^0\right) x_1^2 \tag{9}$$

$$x_3 = 1 - x_2 - x_1 \tag{10}$$

Eqs (5) and (7) were solved simultaneously for $p_{O_2}^0$ and p_T^0 as functions of temperature and $p_{O_2}^\infty$ with the mass transfer parameter γ assumed equal to unity. The fractions x_1, x_2, and x_3 are functions of p_T^0 through Eqs (8) - (10).

Except for reaction (D), the heats and entropies of the above reactions have been taken from the work of Burns et al (11), whose experiments were conducted over a temperature range just in the middle of the range investigated in the present work. The thermochemical properties of reactions (B) - (E) are shown in Table 1.

The calculated ratios of the surface-to-bulk oxygen partial pressures are shown in Fig 1. The oxygen partial pressure at the MoO_2 surface is less than 0.1% of the bulk partial pressure under all conditions of the experiments. Therefore, there are no equilibrium restrictions on the diffusion-controlled oxidation rate. In the regime of complete control of the process by gas phase transport, the partial pressure of oxygen at the surface is effectively zero and the rate is simply given by $k_{gO_2} p_{O_2}^\infty$.

We note a crucial difference between the $Si\text{-}O_2$ system studied by Wagner (10) and the $Mo\text{-}O_2$ system. Ignoring product polymerization which complicates the present case, Eq(5) is equivalent to the transport restriction developed by Wagner. In the $Si\text{-}O_2$ system, the volatile oxide partial pressure is <u>inversely</u> proportional to the square root

of the surface oxygen partial pressure (Eq(12) of ref 10). In the $Mo-O_2$ system, however, the volatile oxide partial pressure is directly proportional to the square root of the surface oxygen partial pressure (Eq(7), again ignoring polymerization). Consequently, in the $Mo-O_2$ system, there is only one surface oxygen partial pressure which is a solution to the combined transport-thermodynamic restrictions. In the case studied by Wagner, two surface oxygen partial pressures satisfied the constraints, which led to hysteresis effects. In addition, if an oxide film is present on the surface, silicon oxidation is equilibrium controlled ($p^0_{O_2}/p^\infty_{O_2} \sim 1$), whereas molybdenum oxidation is diffusion controlled ($p^0_{O_2}/p^\infty_{O_2} \sim 0$). Consequently, the passivity phenomenon which is so striking in the $Si-O_2$ system is not expected in the $Mo-O_2$ system.

Fig 2 shows the computed fraction of oxide polymers for a bulk oxygen pressure of 0.002 atm. The features of these curves are similar to the analagous curves for other bulk oxygen partial pressures up to 0.05 atm. At the low end of the experimental temperature range, the product oxide at the surface is essentially

all trimer. At the high temperature end of the range, the monomer predominates.

The total molybdenum trioxide pressure at which $MoO_2(s)$ dissociates, $\left(p_T^0\right)_{crit}$, is determined by the equilibrium constants for reactions (B), (C) and (E) as:

$$\left(p_T^0\right)_{crit} = K_E + K_B K_E^2 + K_C K_E^3 \tag{11}$$

If the sum of the partial pressures of the molybdenum trioxide polymers established by the diffusion-convection process is less than the value computed by Eq (11), $MoO_2(s)$ is not stable and the surface reverts to molybdenum metal. The trioxide partial pressure at the surface is controlled by the bulk oxygen partial pressure and the transport parameter γ. At each temperature, there is a bulk oxygen pressure at which $\left(p_T^0\right)_{diff}$ calculated froms Eqs (5) and (7) is just equal to $\left(p_T^0\right)_{crit}$. The oxygen partial pressure for which this equality is attained is plotted as a function of temperature on Fig 3 for γ equal to 1.0 and 1.5. The maximum temperature of oxidation experiments at each bulk oxygen partial pressure are also marked on the figure. In all experiments but one, a MoO_2 coat was found on the specimen after oxidation. The one experiment at 2020°K

and $p^{\infty}_{O_2}$ = 0.005 atm (marked with an open circle on Fig 3) emerged as bright metal - no oxide coat had been present during oxidation. This experiment is closest to the curve separating metal and oxide-coated regions of Fig 3. Thus for essentially all of the experiments reported here, the molybdenum surface was coated with a layer of MoO_2, as expected from thermochemical calculations.

Since the vapor pressure of MoO_2 (11) is approximately an order of magnitude smaller than the critical trioxide pressure for disproportionation of MoO_2, the dioxide cannot contribute significantly to volatilization of the molybdenum metal.

The partial pressure of molybdenum trioxide at the surface is less than the vapor pressure of $MoO_3(\ell)$ (12) under all experimental conditions. Consequently, the trioxide is volatilized as rapidly as it is produced on the surface, and the oxide coat on the metal substrate is probably pure MoO_2. Intermediate oxides (e.g., Mo_4O_{11}) have been observed, but are not stable above 1100°K (13).

Experiment

The rotating disk apparatus is shown in Fig 4.

The disk was rotated by a Globe hysteresis synchronous motor at a frequency controlled by an audio oscillator. To prevent overheating of the motor by conduction from the hot disk, the motor drove the shaft through a rubber connector. The bearings for the $\frac{1}{4}$ in. diameter centerless-ground tantalum shaft were mounted in a water-cooled brass support structure. The inductively heated specimen and holder were located about 2 in. above the top bearing. The disk holder was fabricated from molybdenum. It had a depression into which the specimen disks were press-fit and was tapped and threaded to

permit mounting on the tantalum shaft. Galling of the threads at reaction temperatures was prevented by applying a bit of graphite powder to the threaded part. The holder with disk was dynamically balanced for smooth rotation by filing off high spots prior to each run. Speeds up to 15,000 rpm were obtainable. The instability which occurred at higher speeds could not be avoided by shortening the shaft because this caused overheating of the bearings.

The disk specimens were $\frac{1}{2}$ in. diameter and 0.040 in. thick. Both ordinary stock molybdenum sheet and high purity (> 99.9%) material were employed. No detectable difference in the oxidation behavior between the two grades of metal was observed.

Temperature measurement was accomplished by drilling a 0.030 in. hole completely through the disk, through which an optical pyrometer viewed the cavity formed by the inner (threaded) side of the holder, the top of the tantalum shaft, and the underside of the disk. The temperatures so recorded were assumed to represent the disk surface temperature without emissivity corrections. Apparent temperatures measured by sighting on the surface adjacent to the black body hole were unreliable, due to the non-unity emissivity of the surface and to reflection from the heating element of the preheating furnace above the disk. The hot zone of the preheating furnace was held at a temperature of about 1400°C. If the disk temperature was greater than this, the surface appeared cooler than the black body hole. At disk temperatures lower than 1400°C, the black body hole appeared cooler than the adjacent surface. During operation, the surface temperature of the disk varied by less than a degree or two across the diameter. Temperature constancy of ± 5°C could be maintained during the course of an experiment, which lasted from 3 to 45 minutes.

The entire assembly was surrounded by a quartz envelope. A platinum resistance furnace served to preheat the reaction gas to approximately 320°C before it contacted the heated disk. This was done in order to minimize the effects of physical property variations in the boundary layer on the mass transfer coefficients and to avoid condensation of MoO_3 as it diffused through the steep temperature gradient in the boundary layer. However, since a completely isothermal system could not be achieved, an oxide smoke was produced. Because of the nature of the flow patterns over a rotating disk (fluid is sucked in from above the disk and spun off radially), the smoke did not interfere with temperature measurements.

Pre-mixed argon-oxygen or helium-oxygen mixtures of nominal oxygen concentrations of 0.2, 0.5, 2.0 and 5.0 percent were utilized. The precise oxygen content of each gas mixture was obtained mass spectrometrically.

New disks were polished to a high luster by a 15 micron diamond polishing compound, washed in acetone, weighed, and force-fit into the holder. Each disk was used for several runs, but was not repolished between experiments. The holder-specimen combination was screwed onto the shaft, the quartz envelope placed over the assembly and flow of pure argon started. The motor was started and the desired rotational speed established. The furnace and the induction heater were turned on and the system allowed to stabilize at the desired temperature. Once the disk speed and the temperature had attained steady values, the argon flow was quickly switched off and the reactant gas flow directed to the reaction system. After an initial fast flush of reactant gas to sweep out residual argon, the

flow rate was reduced to ~ 950 cc(STP)/min. This rate was necessary to prevent back mixing of the oxygen-depleted gas spun off the disk with the feed gas. Such back mixing significantly reduces the oxygen concentration of the reactant gas and hence the oxidation rate.

The run was terminated by quickly switching off the reactant gas flow and replacing it with a fast flush of either pure argon or a mixture of 4% hydrogen in helium. The disk was allowed to rotate 3 - 5 min at the reaction temperature in the quench gas. After cooling, the holder was removed from the shaft and the disk pried out by screw pressure. If the quench gas was pure argon, the oxide coat on the surface appeared bluish in color. With the hydrogen-helium quench gas, the oxide coat was reduced to a dull gray, easily scratchable elemental molybdenum coat. The disk was re-weighed to determine its weight loss during the experiment.

The weight loss data were converted to an oxidation rate $\dot{m}$ expressed as grams of molybdenum per cm^2 and per second. The oxidation rate was measured as a function of the disk temperature, bulk oxygen partial pressure and disk speed over the ranges shown in Table 2. The weight loss was linear in time under all conditions.

Results

Unless the gaseous oxide product acts as a poison on the surface kinetics, product transport through the boundary layer cannot exert a controlling influence on the oxidation rate. The previous discussion of the thermochemistry of the surface reaction showed that the concentration of oxygen in the gas at the surface is

essentially zero if the reaction is limited by oxygen transport. Under these conditions, the rate is determined by the fixed oxygen driving force for mass transfer, namely $p_{O_2}^{\infty} - 0$. There is no such restriction on the product oxide driving force, and the concentration of gaseous trioxide at the disk surface assumes a value sufficient to remove the oxide produced by the reaction. If $p_{O_2}^{0} << p_{O_2}^{\infty}$, Eq (5) alone determines the partial pressure of the trioxide at the disk surface. If the diffusion coefficient of the product oxide is much smaller than that of oxygen (i.e., $\gamma < 1$), the partial pressure of the trioxide at the surface is merely increased to provide the driving force necessary for product removal.

The oxidation process is assumed to consist of series resistances due to gas phase diffusion-convection of oxygen through the inert gas boundary layer on the rotating disk and surface chemical reaction. The oxidation rate may be written as:

$$\dot{m} = \left(\frac{2}{3}M_{Mo}\right) k_{gO_2} \left(p_{O_2}^{\infty} - p_{O_2}^{0}\right) \tag{12a}$$

and

$$\dot{m} = k_R \left(p_{O_2}^{0}\right)^n \tag{12b}$$

where M_{Mo} is the atomic weight of molybdenum, k_R is the phenomonological rate constant for the surface reaction and n is the order of the reaction with respect to oxygen partial pressure at the surface. The rate constant is assumed to be of the Arrhenius type:

$$k_R = A\, e^{-E_a/RT_0} \tag{13}$$

where A is the preexponential factor, E_a is the activation energy, and T_0 is the disk temperature.

At high temperatures, k_R becomes very large and $p^0_{O_2}$ approaches zero. This is the regime of complete diffusional control in which the oxidation rate is given by:

$$\dot{m}_{DC} = \left(\frac{2}{3}M_{Mo}\right) k_{gO_2} \, p^{\infty}_{O_2} \tag{14}$$

It is known from the theory of rotating disk convection-diffusion that the mass transfer coefficient of a dilute species with a temperature gradient in the boundary layer may be written as (9, 14):

$$k_{gO_2} = \left[\frac{1}{RT_0}\left(\frac{\Omega D_0}{2\pi}\right)^{1/2}\right]\left[\left(\frac{D_0}{D_f}\right)^{1/2} \frac{T_f}{T_0}\right] \tag{15}$$

where R is the gas constant, Ω is the disk speed in radians/sec, and D_0 is the diffusion coefficient of oxygen in the inert diluent at the temperature of the disk surface. The subscript 0 denotes properties at the disk surface temperature and f denotes the film temperature, taken to be the mean of the disk temperature and the bulk reactant gas temperature. The first bracketed term in Eq (15) is the theoretical expression for the mass transfer coefficient if the gas phase is isothermal. This term is derived directly from the governing conservation equations, with no assumptions except for approximation of the axial velocity profile on the disk by linear function. This simplification reproduces the exact solution to within 1% at the Schmidt numbers of interest here (14).

The second bracketed term in Eq (15) approximately accounts for the effect of temperature-induced property variations on the mass transfer rate. It assumes that the Schmidt number and the product of gas density and gas viscosity may be considered constant

in the variable property conservation equations. These two parameters consist of two transport properties whose variation with temperature are in opposite directions (14). Variable property and other effects due to non-diluteness are not accounted for by the second bracketed term of Eq (15). These will be discussed later.

If D_0 varies as the square of the absolute temperature, the mass transfer coefficient is independent both of temperature level and of temperature difference through the boundary layer. This behavior is approximately followed by the oxygen-helium and oxygen-argon mixtures, in which the diffusion coefficients vary as the 1.8 and 1.7 power of the absolute temperature, respectively. Between 1300°K and 1900°K, the isothermal mass transfer coefficient decreases by 8% for argon diluent and 6% for helium diluent. For a bulk gas temperature of 600°K, the variable property factor for argon diluent is 0.95 at a disk temperature of 1300°K and 0.93 at a disk temperature of 1900°K. The analagous figures for helium diluent are 0.97 at 1300°K and 0.95 at 1900°K. Since these variations are less than the precision of the data (which was about ± 15%), the mass transfer coefficient may be considered independent of disk temperature. The partial pressure of oxygen at the disk surface can then be calculated from measured values of $\dot{m}$ and $\dot{m}_{DC}$ by Eqs (12a) and (14):

$$p_{O_2}^{0} = p_{O_2}^{\infty} \; (1-\dot{m}/\dot{m}_{DC}) \tag{16}$$

$\dot{m}_{DC}$ was obtained from experiments at temperatures high enough that the oxidation rate was temperature independent. The diffusion-controlled limit theoretically predicted to be temperature-independent was verified in all gas mixtures studied.

No information on any of the parameters of the surface reaction can be obtained for temperatures in excess of $\sim$ 1400°K, since in this region $\dot{m}$ was so close to $\dot{m}_{DC}$ that evaluation of $p^0_{O_2}$ by Eq (16) was very inaccurate.

Reaction Order

The order of the surface reaction was determined by logarithmically plotting the oxidation rate against the surface oxygen partial pressure computed by Eq (16). A typical plot is shown in Fig 5, and the reaction order obtained from measurements at temperatures below the limit of complete diffusion control are shown in Table 3. Within the precision of the data, the reaction is first order with respect to oxygen partial pressure. Note that the overall oxidation process is also first order at temperatures greater than 1400°K as well, since convective-diffusion is a first order process.

Activation Energy

Having determined the reaction order, the rate constant k_R was obtained from Eq (12b) with n = 1. Fig 6 shows an Arrhenius plot of the data for the 0.5% oxygen in helium reactant gas mixture. The closed circles are the raw weight loss data, but do not represent constant oxygen pressure because $p^0_{O_2}$ differs from 0.005 atm according to Eq (16). When the proper oxygen pressure is utilized (by dividing the measured rates by $1 - \dot{m}/\dot{m}_{DC}$), the corrected rates fall on a good straight line. The horizontal line on the figure represents the experimental diffusion-controlled limit, which for helium diluent, begins at $\sim$ 1650°K. Analogous Arrhenius plots for the experiments utilizing argon diluent were similar in all respects

to the helium diluent data shown in Fig 6 except that the diffusion controlled regime began at ∿ 1500°K (because of the lower diffusivity of oxygen in argon than in helium). The kinetic parameters determined from the five different reactant gases investigated are listed in Table 4. The reason for the anomolous behavior in the 2% oxygen in argon series of experiments is not clear, but may have been due to faulty experimentation since this series was the first attempted. Excluding this set of measurements, the parameters of the surface reaction for 1100<T<1400°K are:

$$E_a = 40 \pm 1 \text{ kcal/mole}$$

$$A = (2.7 \pm 0.5) \times 10^4 \text{ gms/atm-cm}^2\text{-sec}$$

$$n = 1.02 \pm 0.03$$

The range of oxygen partial pressures to which these parameters apply may be estimated as follows. The maximum partial pressure investigated was 0.05 atm. Since much of the data upon which the kinetics are based were obtained under partially diffusion-limited conditions, the minimum surface partial pressure [is estimated to be 5×10^{-4} atm.]. These parameters refer to oxygen attack of the MoO_2 coat, not molybdenum metal. The 40 kcal/mole activation energy is considerably higher than the value of ∿ 23 kcal/mole found by previous workers (7). We believe that the activation energies measured by previous studies in the high total pressure region (3-6) were obscured by gas phase diffusional resistance, which has been properly accounted for in the present work. Had the procedure utilized by Gulbransen et al (4) (measuring the activation energy from the straight portion of the Arrhenius plot of the raw data been

followed, the activation energy from our data would have been $\sim$ 27 kcal/mole.

Direct comparison of the present kinetic parameters with those of Rosner and Allendorf (1) and Berkowitz-Mattuch et al (2) is not possible, since the surface in the latter low pressure experiments may have been bare molybdenum metal rather than the oxide coat characteristic of high pressure oxidation.

The Diffusion-Controlled Region

The oxidation rates at temperatures above 1500°K in argon and 1650°K in helium were independent of temperature and represent complete limitation by gas phase diffusion. The experimental rates per unit oxygen partial pressure taken from the plateaus such as the one shown in Fig 6 are listed in Table 5. For comparison, the theoretical rates calculated from Eqs. (14) and (15) are also shown in the table. The theoretical rates were computed for a bulk gas temperature of 600°K and disk temperatures of 1500°K for argon and 1650°K for helium. Diffusion coefficients of oxygen in the two inert gases were computed from kinetic theory using force constants for the Lennard-Jones intermolecular potential function obtained from gas viscosity data (14).

The experimental rates average ~ 15% greater than the theoretical predictions. This is the same order of discrepancy observed in the germanium-iodine system (9), and is probably largely due to edge effects caused by attack around the rim of the disk. The agreement on the whole is quite satisfactory, and demonstrates that:

(1) The theoretical behavior of a rotating disk system can be realized experimentally at temperatures as high as 2000°K.

(2) The oxygen partial pressure at the disk surface in the diffusion controlled regime is zero, as predicted from the thermochemistry of the reaction.

(3) The $\frac{3}{2}$:1 O_2 to Mo stoichiometry, assumed in reaction (A) and implicit in the theoretical rate expression of Eq (14), is correct.

(4) The MoO_2 scale does not retard oxidation.

The experimental results in Table 5 exhibit a distinct decrease as the oxygen pressure is increased. This effect is probably real,

and due to the loss of "dilute" character of the reactant gas. This includes the effect of variable density in the conservation equations due to the change of average molecular weight through the gas boundary layer and the effect of interfacial velocity due to the oxidation process. The former tends to increase the diffusional rate as the bulk oxygen partial pressure is increased (14), whereas the latter tends to reduce transfer by thickening the boundary layer (9). These effects are most severe for the 5% oxygen in argon case, and, because of the low atomic weight of helium, in the 0.5% O_2 in He experiments. In addition, the influence of thermal diffusion driven by the $\sim$ 2000°K/cm temperature gradient in the boundary layer has not been considered.

Since the flow geometry is one in which the heated disk is facing upward, the disk-to-gas temperature difference can generate appreciable natural convection transfer. Simple calculations in which the magnitude of the heat transfer Nusselt numbers for natural and forced convection were compared suggest that the forced convection heat transfer coefficient is $\sim$ 4 times larger than the natural convection heat transfer coefficient at a disk speed of 9600 rpm and a disk temperature of 1700°K. In this calculation, the gas phase was assumed to be argon at 600°K. Experiments were performed at disk speeds from 1500 to 15,000 rpm to determine the effect of natural convection. The results, shown in Fig 7, suggest that natural convection is significant below 9000 rpm, but that the mass transfer rate obeys the $\sqrt{\Omega}$ relation predicted by Eq (15) at higher speeds. All experiments other than those shown in Fig 7 were conducted at 9600 rpm.

Reaction Mechanism

Because of the complexity of the surface processes when both scale formation and volatilization occur, conclusive determination of a mechanism is not possible. However, the following factors serve to constrain the number of alternatives:

(1) The rate depends upon the first power of the oxygen partial pressure at the specimen surface.

(2) The activation energy is independent of temperature and reactant gas composition.

(3) $\frac{3}{2}$ moles of oxygen are required to remove one gram atom of molybdenum.

(4) A coat of MoO_2 separates the metal substrate from the reactant gas, but diffusional processes in the coat are not rate limiting.

The following mechanism is consistent with these observations.

In the first step, oxygen is dissociatively adsorbed on the oxide surface:

$$O_2(g) \rightarrow 2\,O(ads) \qquad (H)$$

Subsequently, and oxygen adatom reacts with MoO_2 to produce the trioxide:

$$O(ads) + MoO_2 \rightarrow MoO_3(ads) \qquad (I)$$

The adsorbed MoO_3 desorbs as one of the polymeric gaseous oxide species:

$$mMoO_3(ads) \rightarrow (MoO_3)_m(g) \qquad (J)$$

Molybdenum dioxide is believed to be a n-type semiconductor

oxide (15). We assume it to be of the oxygen-deficient type for this discussion. Adsorbed oxygen acquires a mobile electron from the lattice to form the adsorbed ion:

$$O(ads) + e^- = O^-(ads) \qquad (K)$$

The adsorbed oxygen ion moves into an oxygen vacancy at the surface and becomes part of the lattice:

$$O^-(ads) + \boxed{\dot{O}}_1 = O_\ell^{-2} \qquad (L)$$

The symbol $\boxed{\dot{O}}$ represents an anion vacancy to which an electron is attached and O_ℓ^{-2} denotes an ordinary lattice oxygen ion. The subscript 1 denotes the gas-oxide interface. At the metal-oxide interface (denoted by the subscript 2), molybdenum reacts with an oxygen ion to release anion vacancies and charge carriers:

$$Mo(s) + 2O_\ell^{-2} = MoO_2 + 2\,\boxed{\dot{O}}_2 + 2e^- \qquad (M)$$

The oxygen vacancies and mobile electrons migrate to the surface to supply reaction (L):

$$\boxed{\dot{O}}_2 \rightarrow \boxed{\dot{O}}_1 \qquad (N)$$

If all steps are in equilibrium, reactions (H) - (N) reduce to reaction (A).

The above sequence of steps is identical to the well-known Wagner mechanism describing thick scale growth for this type of oxide except for volatilization reactions (I) and (J).

We need to identify a rate-controlling step in this sequence. One of reactions (H), (I), or (J) must be the rate controlling step. If all three were fast and in equilibrium, the partial

pressure of oxygen and the polymeric trioxides at the surface would be related by Eq (7). However, the mass transfer relation of Eq (5) must always be satisfied. It was shown previously that when Eqs (5) and (7) must be simultaneously satisfied the surface partial pressure of oxygen is very close to zero and the entire process is limited by gas phase diffusion. Since the rate is not gas diffusion limited in the temperature region where $\dot{m} < \dot{m}_{DC}$, reactions (H), (I), and (J) cannot all be in equilibrium in the reaction limited region.

If reaction (H) and (J) were in equilibrium and reaction (I) was controlling, the rate would vary as the square root of the oxygen partial pressure, contrary to the observed first order dependence.

If reactions (H) and (I) were at equilibrium and reaction (J) rate controlling, the rate would vary as the oxygen partial pressure to some power between $\frac{1}{2}$ and $\frac{3}{2}$, depending on the polymer desorbed. The observed first order behavior would occur only if the dimer were the sole gaseous oxide desorbed from the surface, which is unlikely on thermodynamic grounds.

Consequently, we conclude that reaction (H) is the rate controlling surface step in the temperature range 1100 - 1400°K. This step is first order in oxygen partial pressure (provided that the fractional coverage of the active sites on the oxide surface by O_{ads} is small, which is expected if reactions following (H) are rapid and the system is far from equilibrium). The slight increase in reaction order as the temperature is decreased (see Table 3) may be due to partial control of the overall reaction by desorption of the trimer.

Gulbransen et al (4) also concluded that oxygen adsorption controlled the rate on the basis of comparison of a single experiment at 1170°K and 0.1 atm oxygen pressure with the absolute

rate theory expression for activated adsorption to a mobile adsorbed state:

$$R_{O_2} = \frac{P^0_{O_2}}{N_{Av}\sqrt{2\pi M_{O_2} RT_0}} e^{-E_a/RT_0} \tag{17}$$

where N_{Av} is Avogadro's number and M_{O_2} is the molecular weight of oxygen. As noted by Schryer (16), the pre-exponential term in Eq (17) is identical to the kinetic theory rate of impingement of oxygen on the surface. Multiplying Eq (17) by $\frac{2}{3}M_{Mo}$ to give the rate in terms of the units used in this work yields a pre-exponential factor of

$$A = 15 \text{ gm/cm}^2\text{-sec-atm}$$

which is 2000 times smaller than we obtained from our data. The discrepancy may be due to increasing availability of surface sites suitable for dissociative adsorption as the temperature is increased. The active sites may be associated with surface defects (17). If this were so, the right hand side of Eq (17) would be multiplied by $A_s e^{-E_s/kT}$, which represents the fraction of the surface sites which are active. E_s is the energy of formation of the active sites and $A_s \sim 2000$, as suggested by the ratio of the observed pre-exponential factor and that obtained from kinetic theory collision rate. This value of A_s is of the same order as that estimated for Schottky disorder in bulk solids (18).

The substantial activation energy for dissociative chemisorption would not be expected on a metal, where the binding is relatively uniform over the surface. In the case of a non-metal, however, the discreteness and wide separation of the binding sites implies that both atomic partners of the adsorbing molecule cannot strongly interact with two binding sites without being vibrationally excited

(19). Molecular dissociation may be restricted by the appreciable separation of the binding sites on the oxide surface. An activation energy of 40 kcal/mole is not unreasonable if vibrational excitation is a prerequisite to dissociative adsorption. However, if the adsorption process is connected with the temperature-dependent concentration of defects on the surface, the measured activation energy represents the sum of a normal activation energy for chemisorption and the formation energy of the surface defect.

Role of the Oxide Coat

Accepting reaction (H) as the rate-determining step, the thickness of the oxide coat on the surface may be determined by an analysis similar to that recently suggested by Rosner and Allendorf (20). For convenience, we assume the gaseous trioxide to be all trimer, which is favored thermodynamically in the low temperature region where information on the surface processes is available. Since reactions (I) and (J) are in equilibrium, the concentration of O(ads) is proportional to the cube root of the trimer partial pressure. If the surface steps (K) and (L) are also in equilibrium, the concentration of oxygen vacancies at the surface is proportional to the inverse square root of the O(ads) concentration. Thus equilibrium of reactions (I) through (L) requires that:

$$\boxed{\dot{O}}_1 = K\left(p_3^0\right)^{-1/6} \tag{18}$$

where K is a combination of the mass action constants for the reactions involved.

If equilibrium is also attained at the metal-oxide interface,

$$\boxed{\dot{O}}_2 = \sqrt{K_M} \tag{19}$$

where K_M is the equilibrium constant for reaction (M).

The rate of diffusion of lattice oxygen ions from the gas-oxide surface to the metal-oxide interface is equal in magnitude but opposite in direction to that of oxygen vacancies:

$$R_d = \frac{D_{\boxed{O}}\left\{\boxed{\dot{O}}_2 - \boxed{\dot{O}}_1\right\}}{\xi} = \frac{k}{\xi} \tag{20}$$

where R_d is the rate of oxygen transport from the surface to the metal-oxide interface in gm atoms/cm^2-sec, $D_{\boxed{O}}$ is the diffusion coefficient of oxygen vacancies in the scale and ξ is the scale thickness. The product of the diffusion coefficient and the

driving force is the scaling constant, k. If the vacancy concentration at the gas-oxide surface is much smaller than that at the metal-oxide interface, the scaling constant is independent of surface conditions or coat thickness.

Adjustment of the scale thickness to the experimental conditions can best be seen by examining the growth kinetics during the initial stages of the oxidation process. Suppose the specimen is initially either bare metal or covered with an oxide coat. Let a constant rate of supply of oxygen adatoms to the surface from chemisorption reaction (H), R_O, commence at zero time. By a mass balance over a volume containing the gas-oxide interface, the rate at which oxygen atoms leave the surface in the form of the product trioxide is equal to the difference between R_O and R_d.

The growth of the MoO_2 film is governed by the scaling law:

$$\frac{1}{V_{ox}} \frac{d\xi}{dt} = \frac{1}{2} R_d - (R_O - R_d) = \frac{3}{2} \frac{k}{\xi} - R_O \tag{21}$$

where V_{ox} is the molar volume of MoO_2. The usual parabolic scaling law is recovered if the volatilization term $(R_O - R_d)$ is absent. The solution to Eq (21) may be obtained by standard methods. At long times, a constant thickness equal to $3k/2R_O$ is approached. The characteristic time of approach to steady state is $k/V_{ox}R_O^2$. If the initial scale thickness is larger than the steady state value, the coating thickness decreases with time. If the specimen is bare metal at the start, the coat grows in time until the steady state thickness is attained. Expressing the rate of oxygen atom adsorption in terms of the steady state rate of metal removal, the coating thickness during the oxidation can be written as:

$$\xi_{ss} = \frac{kM_{Mo}}{2\dot{m}} = \frac{kM_{MO}}{2k_R p^0_{O_2}} \tag{22}$$

Thus the diffusional properties of the MoO_2 scale influence the time required to achieve the steady state coat and the thickness of the coat in the steady state, but do not affect the overall rate of oxidation, which is controlled by the rate of dissociative adsorption of oxygen on the oxide surface. Since departures from the linear oxidation law were not observed, the oxide scale must have achieved its steady state thickness very quickly compared to the length of time the experiments were conducted.

Acknowledgement

The authors wish to thank Dr. Amos Newton for providing mass spectrometric analyses. The comments and suggestions of D. Rosner are also gratefully acknowledged. This work was performed under the auspices of the U.S. Atomic Energy Commission.

1. Rosner, D.E. and H.D. Allendorf, J. Chem. Phys. 40, 3441 (1964).

2. Berkowitz-Mattuck, J.B., A. Buchler, J.L. Engelke, and J.N. Goldstein, J. Chem. Phys. 39, 2722 (1963).

3. Schryer, D.R. and J.L. Modisette, Planetary and Space Science 3, 31 (1961).

4. Gulbranson, E.A., K.F. Andrew, and F.A. Brassart, J. Electrochem Soc., 110, 952 (1963).

5. Semel, Jr., J.W. in High Temperature Materials, R.F. Hekemann and G.M. Ault, Eds., p. 510, John Wiley, New York (1959).

6. Berkowitz, J., Wright Patterson, AFB Report ASD TDR 62-203, Part I (1962).

7. Rosner, D.E. and H.D. Allendorf, J. Electrochem Soc., 111, 759 (1964).

8. Rosner, D.E., AIAA Journal 2, 593 (1964).

9. Olander, D.R., I&EC Fund. Quart. 6, 178, 188 (1967).

10. Wagner, C., J. Appl. Phys. 29, 1295 (1958).

11. Burns, R.P., G. DeMaria, J. Drowart, and R.T. Grimley, J. Chem. Phys. 32, 1363 (1960).

12. Gulbranson, E.A., K.F. Andrew, and F.A. Brassart, J. Electrochem Soc., 110, 242 (1963).

13. Kihlborg, L., Acta Chemica Scand. 13, 954 (1959).

14. Schofill, J., (Ph.D. Thesis) UCRL-19029 (1969).

15. Hauffe, K., "Oxidation of Metals", Plenum Press, New York (1965).

16. Schryer, D.R., J. Electrochem Soc., 111, 757 (1964).

17. Parravano, G., Catalysis Revs. 4, 53 (1970).

18. Jost, W., Diffusion in Solids, Liquids, Gases, Academic Press, p. 116 (1960).

19. Ehrlich, Gert, J. Chem, Phys., 31, 1111 (1959).

20. Rosner, D.E. and H.D. Allendorf, J. Phys. Chem. 74, 1829 (1970).

Table 1. Thermochemistry of the Mo-O_2 System

Reaction	$\Delta H^0_{1600°K}$, kcal/mole	$\Delta S^0_{1600°K}$, eu	ref
B	- 110.2	- 42.1	10
C	- 222.8	- 88.6	10
D	137.1	39.3	*
E	121.8	46.4	10

* Kubachewski, O. and E. Evans, "Metallurgical Thermochemistry", Pergamon Press (1967); Mc Iver, E. J. and S. S. Teale, AERE-R 4942 (1965); also data quoted in ref 4.

Table 2, Experimental Conditions

Disk Temperature: 1100 - 2000°K
Gas Temperature: ~600°K

Gas Pressure (total): 1 atm
Oxygen Concentration: 0.2 to 5.0%
Diluent Gas: argon or helium

Disk Speed: up to 15,000 rpm

Table 3. Reaction Order

T_0, °K	n
1150	1.06
1225	1.02
1300	0.99
1375	0.99
Avg	1.02 ± 0.03

Table 4. Kinetic Parameters

Oxygen Concentration	E_a (kcal/mole)	A (g/atm-cm^2-sec) x 10^{-4}
	Argon diluent	
0.2%	40	3.5
0.5%	40	2.2
2.0%	(49)	(82.0)
5.0%	39	2.3
	Helium diluent	
0.5%	40	2.6

Table 5. Diffusion Controlled Rates

$$\left(\frac{2}{3}M_{Mo}\right)k_{gO_2} = \dot{m}_{DC}/p^{\infty}_{O_2}, \quad (g/atm\text{-}cm^2\text{-}sec) \times 10^2$$

Nominal Oxygen Concentration	Experimental	Theoretical
	Argon	
0.2%	1.25 ± 0.10	1.06
0.5%	1.20 ± 0.04	
2.0%	1.12 ± 0.08	
5.0%	1.10 ± 0.02	
	Helium	
0.5%	2.62 ± 0.15	2.12

1. Ratio of the oxygen partial pressures at the surface and in the bulk for gas phase transport controlled oxidation.
2. Fraction of the product oxide at the disk surface in various polymeric forms. 0.2% oxygen in bulk reactant gas.
3. Regions of stability of the MoO_2 scale.
4. Rotating disk apparatus.
5. Plot to determine reaction order. 1225°K and 9600 rpm.
6. Arrhenius plot of oxidation rate data for 0.5% oxygen in helium at 9600 rpm.
7. Effect of disk speed on the oxidation rate in the diffusion-limited regime. Reactant gas 0.5% oxygen in argon.

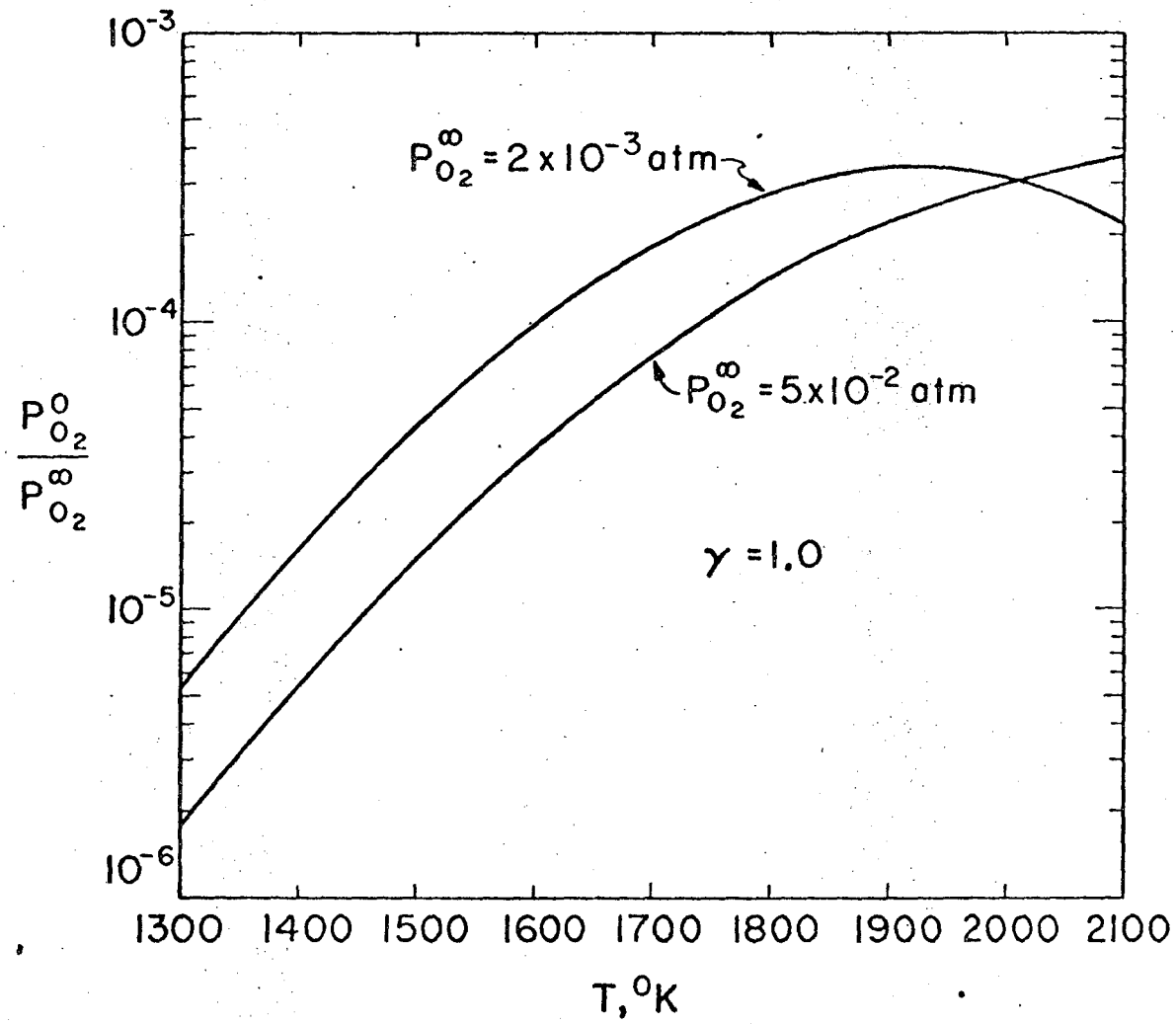

XBL702-2307

Olanders Schofill

Fig. 1

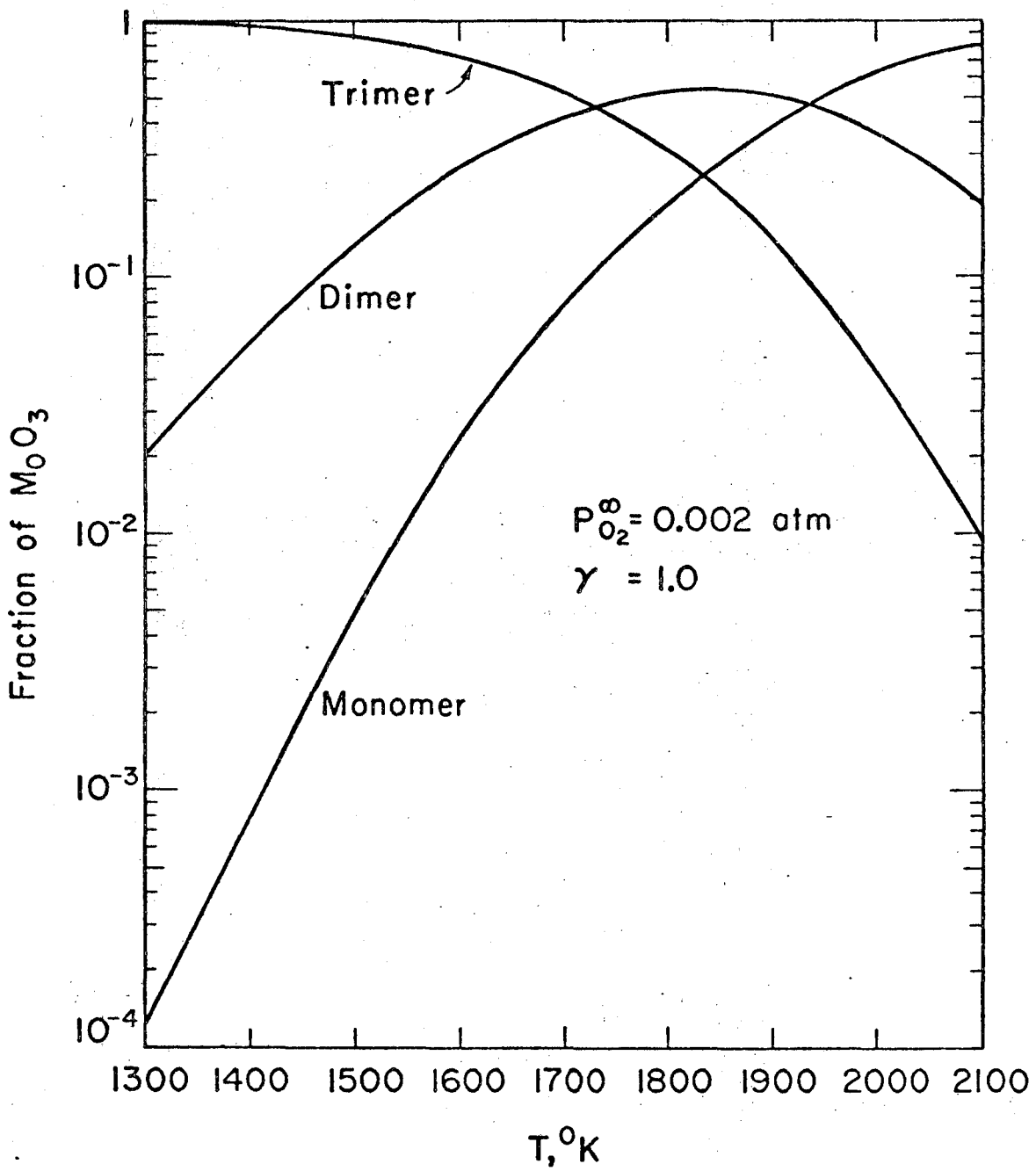

XBL702-2306

Fig 2

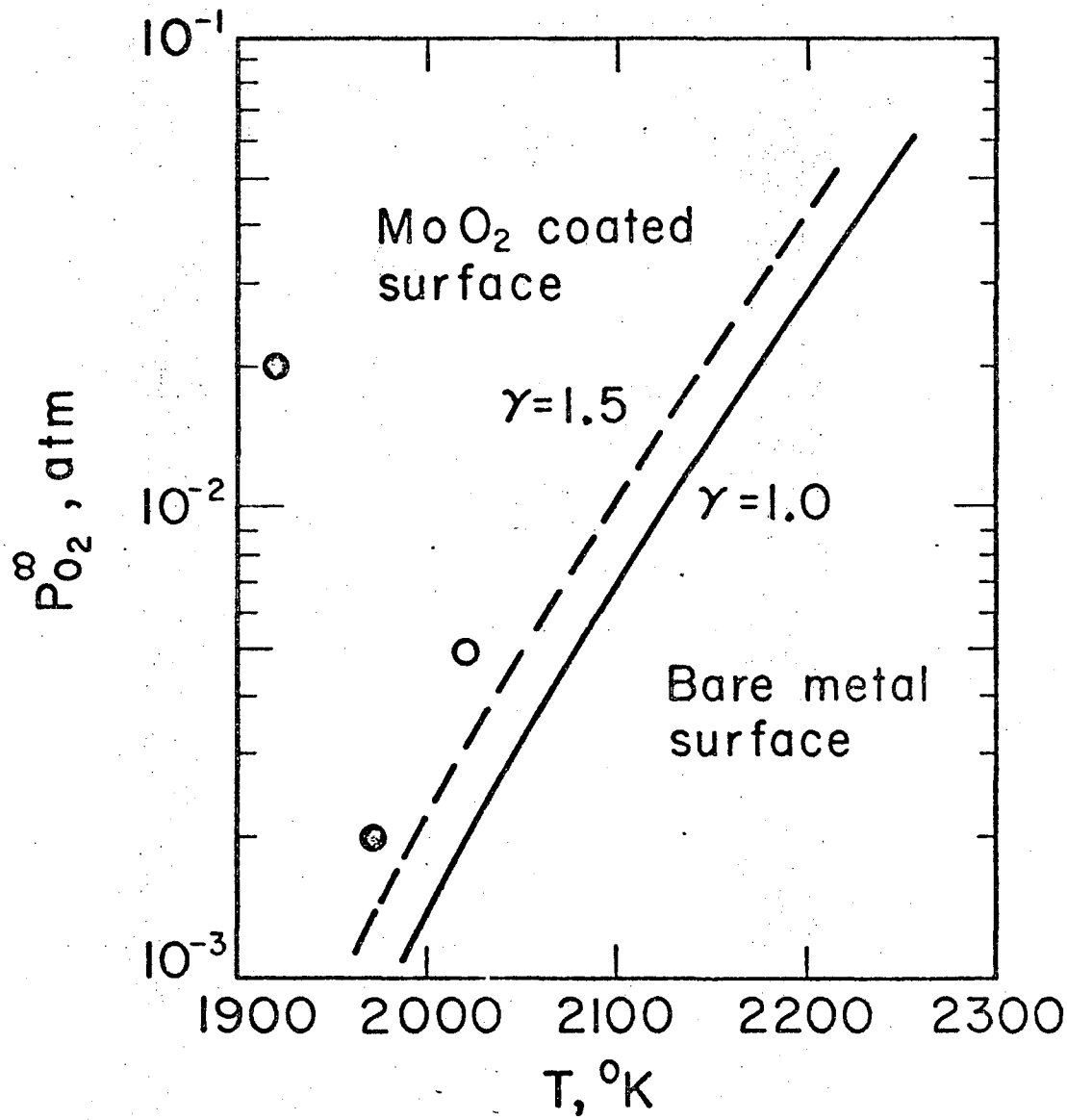

XBL702-2308

Fig 3

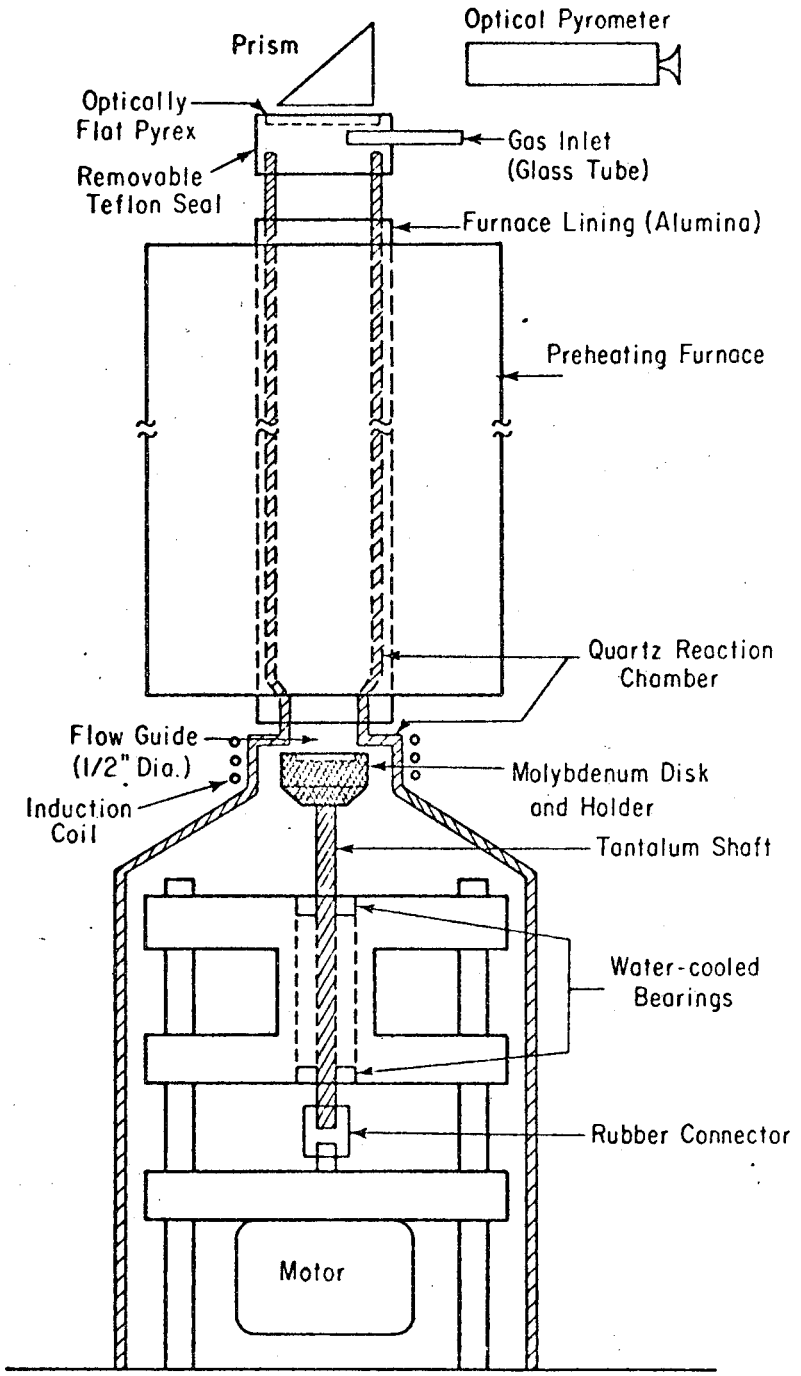

XBL 697-850

Olander + Schofill

Fig 4

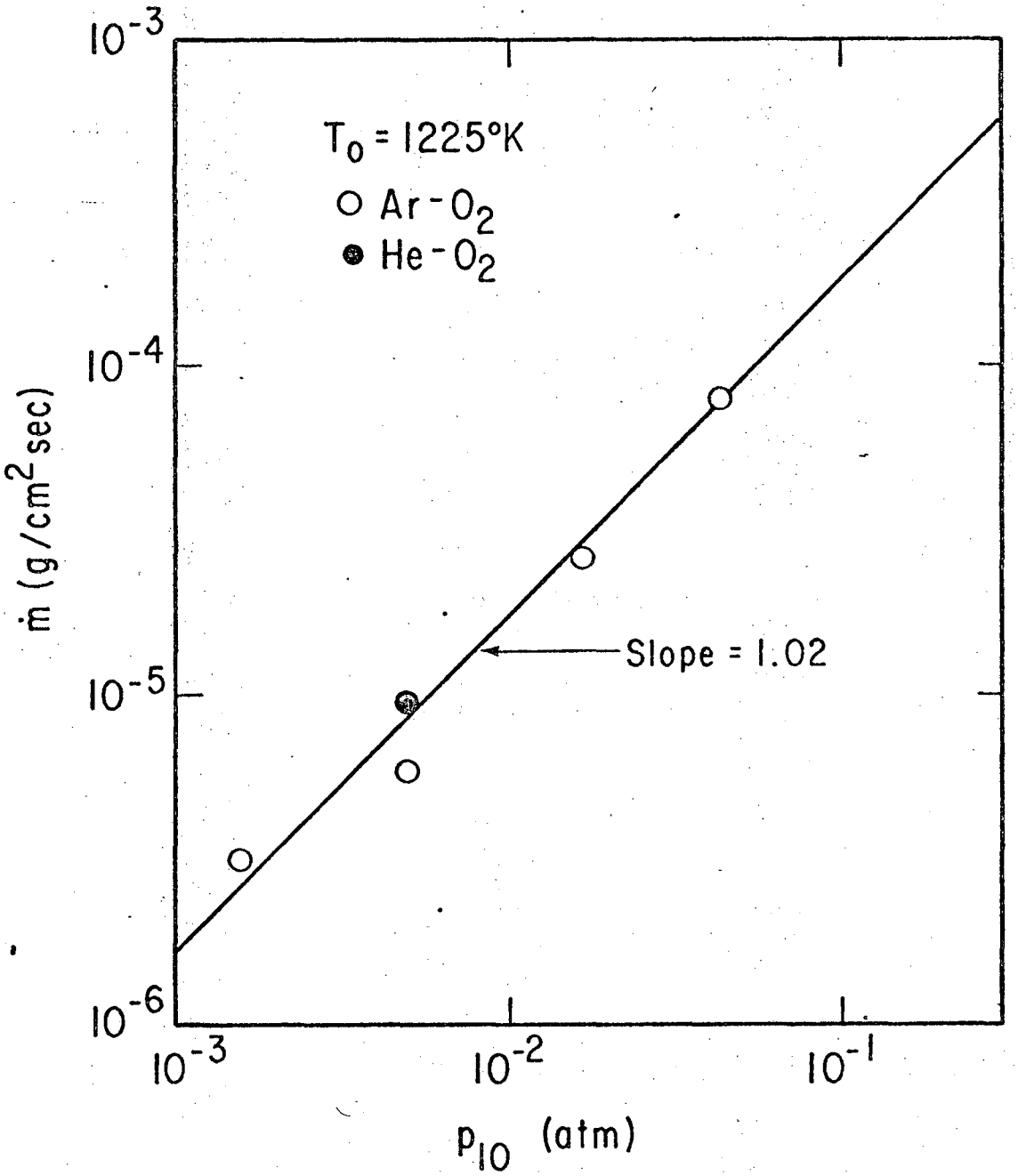

XBL 697-834

Olander & Schotill

Fig 5

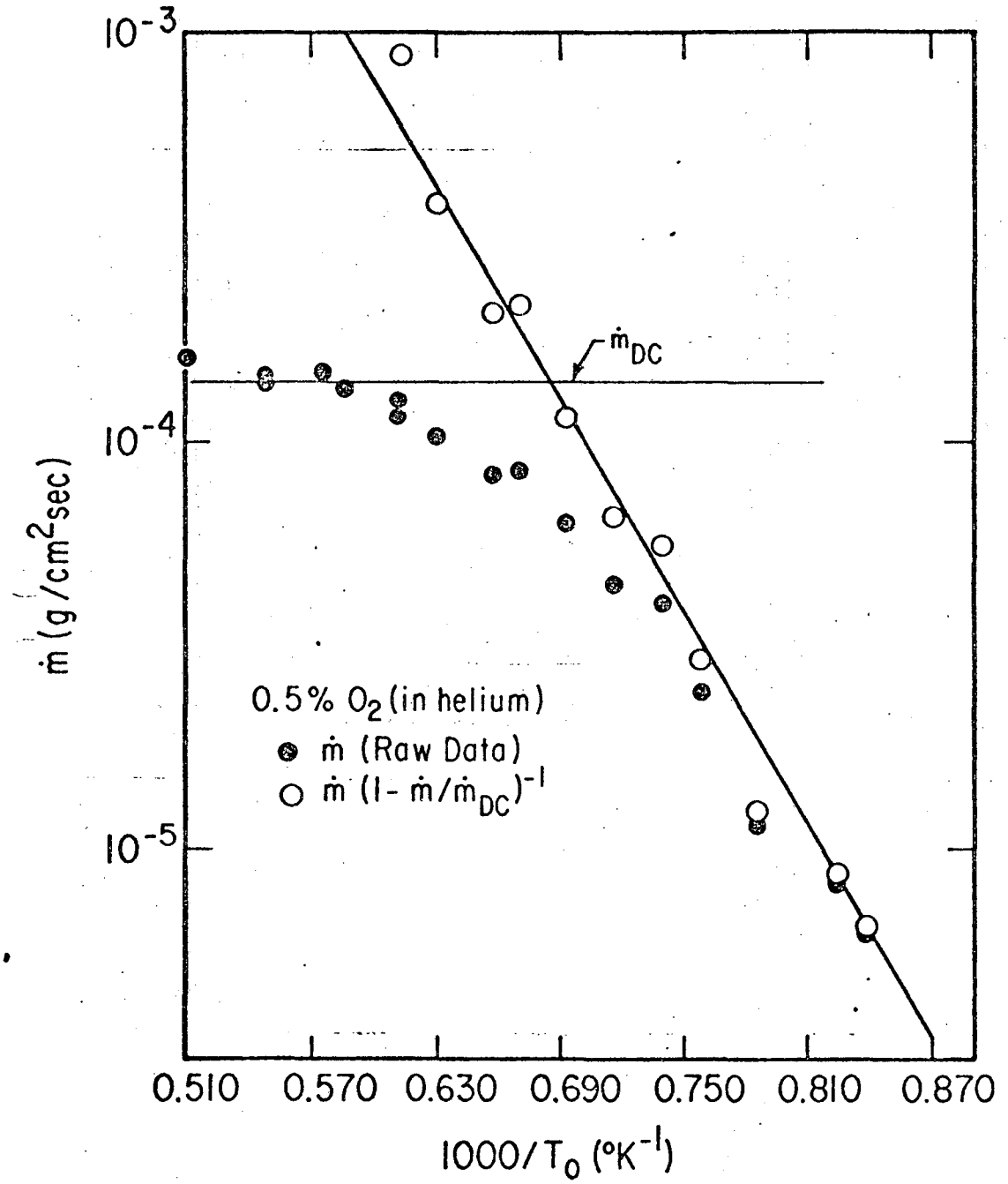

XBL 697-835

Olander & Schotill

Fig 6

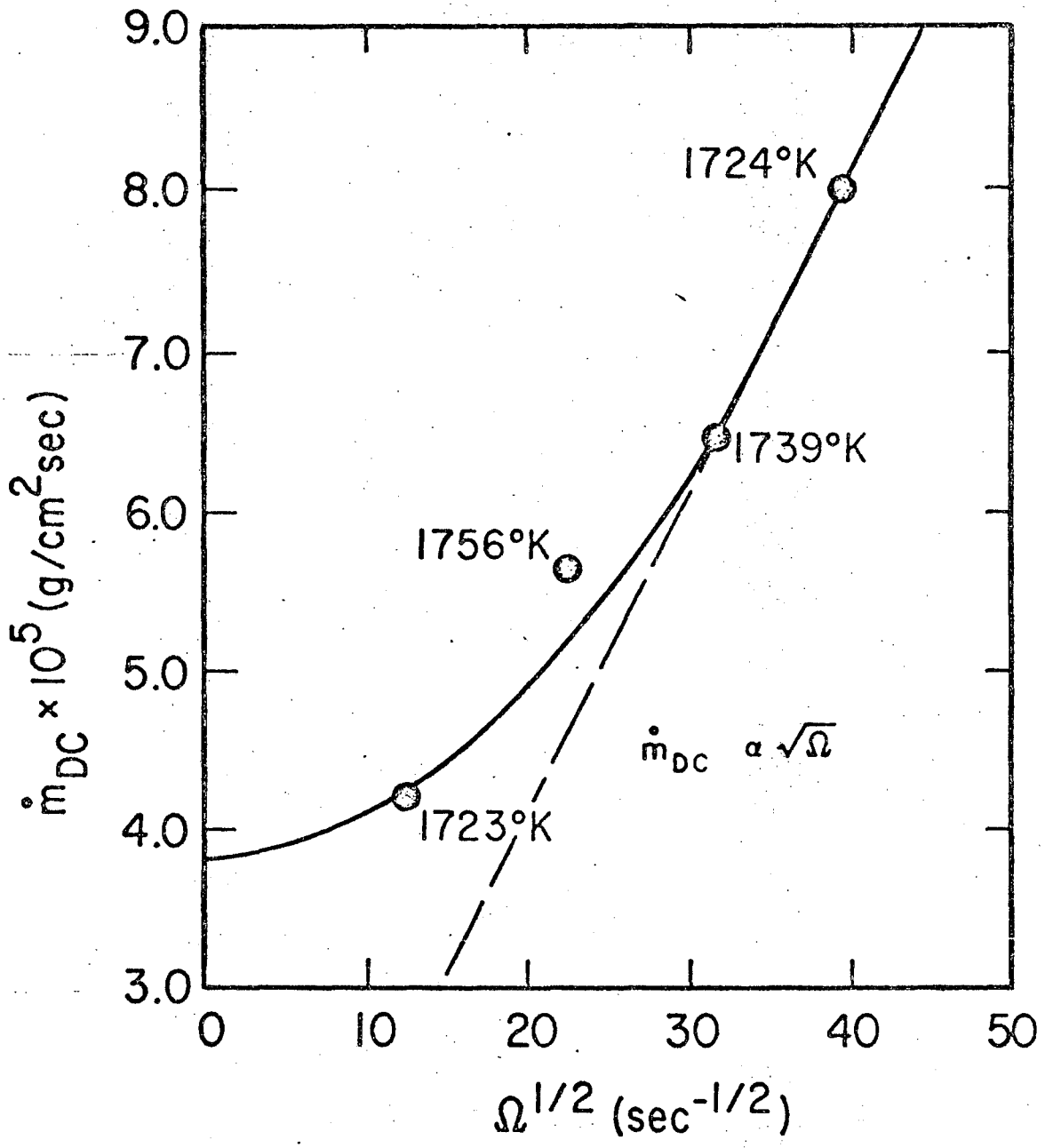

XBL 697-828

Fig 7

LEGAL NOTICE

This report was prepared as an account of Government sponsored work. Neither the United States, nor the Commission, nor any person acting on behalf of the Commission:

A. Makes any warranty or representation, expressed or implied, with respect to the accuracy, completeness, or usefulness of the information contained in this report, or that the use of any information, apparatus, method, or process disclosed in this report may not infringe privately owned rights; or

B. Assumes any liabilities with respect to the use of, or for damages resulting from the use of any information, apparatus, method, or process disclosed in this report.

As used in the above, "person acting on behalf of the Commission" includes any employee or contractor of the Commission, or employee of such contractor, to the extent that such employee or contractor of the Commission, or employee of such contractor prepares, disseminates, or provides access to, any information pursuant to his employment or contract with the Commission, or his employment with such contractor.

TECHNICAL INFORMATION DIVISION
LAWRENCE RADIATION LABORATORY
UNIVERSITY OF CALIFORNIA
BERKELEY, CALIFORNIA 94720